

Nearest Target for Retina Images Based On Canny Edge Detector and Ensemble Classifiers

Mrs.B.Sivaranjani¹, Dr.C.Kalaiselvi²

¹Ph.D. Research Scholar, Department of Computer Science,
Tiruppur Kumaran College for Women, Tiruppur
Assistant Professor, Department of IT, Dr.N.G.P.Arts and Science College, Coimbatore
E-mail: sivi.nair@gmail.com

²Head and Associate Professor, Department of Computer Applications,
Tiruppur Kumaran College for Women, Tiruppur
E-mail: kalaic29@gmail.com

Abstract

For retina problems diagnosing, valuable information to ophthalmologists are provided by Retinal fundus images. Curing rate can be enhanced using early detection and it may prevent blindness. Using retinal fundus images, medical experts diagnosis retinal problems like retinitis pigmentosa and diabetic retinopathy. Mutual Information (MI) optimization is initialized as coarse localization process, where optimization domain is narrowed and local optima are avoided in recent works. In addition, Improved Support Vector Machine (ISVM) technique is used for performing retina image's nearest template and it is used with registration based on area, provides a robust technique. However, proper detection of retina image's edges are not done using these techniques and concerned region's visibility and perceptibility. Performing Retina image's nearest template according to single classifiers leads to degradation in classifier accuracy. So, for avoiding this issue, a four stage framework is proposed in this work. Fuzzy clustering algorithm based noise removal is done in the first phase, where similarity among un-noisy and noisy pixels are computed. Canny edge detection operator based edge detection and enhancement are done at the second stage. Dimension reduction is done in the third stage, where Mutual Information (MI) optimization is initialized as coarse localization process, where optimization domain is narrowed and local optima are avoided. Fuzzy neural network (FNN), Probabilistic neural network (PNN), Adaptive Neuro Fuzzy Inference System (ANFIS) classifier's ensemble is used for computing retina image's nearest template in fourth stage. For STARE dataset, with respect to run time rate, success rate and mean error rate, proposed model's robustness is demonstrated using experimental results.

Keywords: *canny edge detection operator, fuzzy clustering, Retinal fundus images, coarse localization, Mutual Information (MI).*

1. Introduction

Most important human sense is vision. Person's independence and productivity are affected by lacking in vision. Millions of people are affected by retinal diseases and it may result in vision loss, if it not treated and diagnosed in early stages. Glaucoma, age related macular disorder, diabetic retinopathy are the examples of retinal diseases.

This disease can be cured or its onset can be slowed using available early treatment options. Treated patients can get several more vision years in their life. In India, doctor to patient ratio is still low even with large number of hospitals and eye clinics [1,2].

In provincial zones, there is absence of both foundation and accessibility of ophthalmologists. Indeed, even network outreach programs are incapacitated by the absence of prepared work force to successfully screen patients in country regions. Far off picture procurement and symptomatic require significant expense and framework. With progress in innovation and picture investigation, it is conceivable

to robotize the cycle of ailment recognition and allude the patient to the specialist for additional conference.

Various such clinical choice emotionally supportive networks have been grown particularly to analyze diabetic retinopathy, age related macular issue utilizing progresses in advanced picture preparing and AI. Despite the fact that, the exhibition of a significant number of these frameworks are practically identical to human specialists, they are particular to analyze a particular retinal ailment. Huge numbers of these models distinguish, remove and investigate sickness explicit highlights from the retinal picture. Albeit achievable much of the time, the cycle can come up short on bad quality retina pictures without enough unmistakable features[3,4].

For overcoming these issues, fuzzy clustering algorithm based noise removal is done in the first phase, where similarity among un-noisy and noisy pixels are computed. Canny edge detection operator based edge detection and enhancement are done at the second stage. Dimension reduction is done in the third stage, where Mutual Information (MI) optimization is initialized as coarse localization process, where optimization domain is narrowed and local optima are avoided.

In addition, Improved Support Vector Machine (ISVM) technique is used for performing retina images nearest template and it is used with registration based on area, provides a robust technique. However, proper detection of retina image's edges are not done using these techniques and concerned region's visibility and perceptibility. Performing Retina image's nearest template according to single classifiers leads to degradation in classifier accuracy. For avoiding those issues, clustering algorithm based image denosing is performed in first stage [5, 6].

Fuzzy clustering algorithm based noise removal is done in the first phase, where similarity among un-noisy and noisy pixels are computed. Canny edge detection operator based edge detection and enhancement are done at the second stage. Dimension reduction is done in the third stage, where Mutual Information (MI) optimization is initialized as coarse localization process, where optimization domain is narrowed and local optima are avoided. Fuzzy neural network (FNN), Probabilistic neural network (PNN), Adaptive Neuro Fuzzy Inference System (ANFIS) classifier's ensemble is used for computing retina image's nearest template in fourth stage.

2. Related Works

For retina image diseases diagnosis, review about various techniques used are presented in this section.

The inner limiting membrane which is a top most retinal layer in spectral domain optical coherence tomography (SD-OCT) scan is segmented using an automated algorithm proposed by Ramzan et al [2018]. Diagnosis of retinal diseases like glaucoma and macular edema by ophthalmologist are enabled by this segmentation as ILM layer may get affected by this. Correct detection and diagnosing of glaucoma is a foremost purpose behind this segmentation. World Health Organization declared Glaucoma as second common blindness cause and if not treated in early stages, it may cause sever damages.

For glaucoma, considered the Optic-nerve-head (ONH) centered OCT scans. Glaucoma is described as optic nerve head's cupping. Increase in optic cup's diameter ends up in cup to disc diameters (CDR) ratio increase. When compared with normal images, in glaucoma images, in central-cup section, ILM is steeper. So, from ONH or macula centered OCT image volumes, cup is extracted using ILM and they are classified as normal or glaucoma-tic eye.

For retinal images based cataract grading and detection, an automated system is presented by Imran, et al [2019]. Major steps of this technique includes, grading, cataract detection, classifier building, feature extraction and pre-processing and image acquisition. The quality of retinal images are boosted by applying top-bottom hat transformation, green channel extraction and histogram equalization in pre-processing steps. For classifier building, from retinal image, extracted the wavelet and texture features.

For obtaining cataract's better prediction accuracy, RBF (Radial Basis Function) and SOM (Self-Organizing Maps) neural networks combination has been applied. On Tongren dataset, evaluated the SOMRBF neural network with 8030 subjects. They are classified into four classes namely, Severe, Mature, Mild and Normal. For cataract detection, 95.3% accuracy and for grading 91.7% accuracy is proposed by this technique.

For extracting uniqueness-driven saliency according to intensity uniqueness and spatial distributions in images, a new technique is proposed by Zhao, et al [2018]. New saliency feature introduction is a major contribution of this technique. For various problems, without parameter tuning, in various images types, powerful detection can be done using these features.

Retinal image's detection lesions are applied with this technique for evaluating its effectiveness. From malarial retinopathy and diabetic retinopathy's 7 independent public retinal image datasets, four various lesions types namely leakage, micro aneurysms, hemorrhage and exudates are studied. When compared with state-of-the-art techniques, superior performance is shown by proposed technique as indicated in experimental results.

Multiple instance learning (MIL) framework based new methodology is developed by Costa et al [2018] for rectifying these necessity. At image level, on annotations, implicit information are leveraged using this technique. Image classification stages and instance encodings joint optimization is a major contribution made by proposed method when compared with available DR detection systems based on MIL.

Pathological image's highly useful mid-level representations are obtained in this manner. A new loss function enforcing mid-level and appropriate instance representations are used for further enhancing model decisions explain ability. On Messidor, around 90% area under receiver operating characteristic curve (AUC), on DR1, 93% AUC and on DR2, 96% AUC is produced by proposed technique with produced decision's interpretability enhancement. Existing techniques are outperformed by proposed techniques.

From digital fundus images, for detecting cataract, a new automatic cataract detection (ACD) technique is proposed by Pratap and Kokil[2019]. A two class problem is formulated from this cataract detection. Input fundus images are classified as cataract or normal. From singular value decomposition, first 20 singular values are used as features in this proposed ACD technique. Then for classification, support vector machine is applied with these features.

For cataract detection, around 97.78% detection accuracy or testing accuracy is produced. In cataract evaluation, available techniques are outperformed by proposed technique as indicated in obtained results.

The retinal blood vessel's modified directional matched filter parameters are proposed by Raman, et al[2019] for localizing optic disc center. In MATLAB, proposed technique is implemented and using Optic Nerve Head Segmentation Dataset (ONHSD) subset, both abnormal and normal low resolution retinal images are evaluated and around 96.96% average success percentage was produced within 23 seconds.

A new features extraction technique is included in the technique presented by Barua and Hasan [2016]. For proper identification of retinal disease, after the application of segmentation procedure, features are extracted from retinal images. From retinal image, vascular tree is extracted at first and then for generation of features, image is segmented. For ANN classifier training, these features are used via Back propagation algorithm.

A new publicly available High Resolution Fundus (HRF) image dataset is used in experimentation, where described technique is applied on it. Around 97% detection rate is produced for retinopathy, 99% for glaucoma and 99% for healthy condition.

3. Proposed Methodology

Detailed discussion about retina images detection based on proposed model is presented in this section. There are four stages in this model. Fuzzy clustering algorithm based noise removal is done in the first phase. Canny edge detection operator based edge detection is done at the second stage. Dimension reduction is done in the third stage, where Mutual Information (MI) optimization is initialized as coarse localization process. Fuzzy neural network (FNN), Probabilistic neural network (PNN), Adaptive Neuro Fuzzy Inference System (ANFIS) classifier's ensemble is used for computing retina image's nearest template in fourth stage. Figure 1 shows the proposed work's overall architecture.

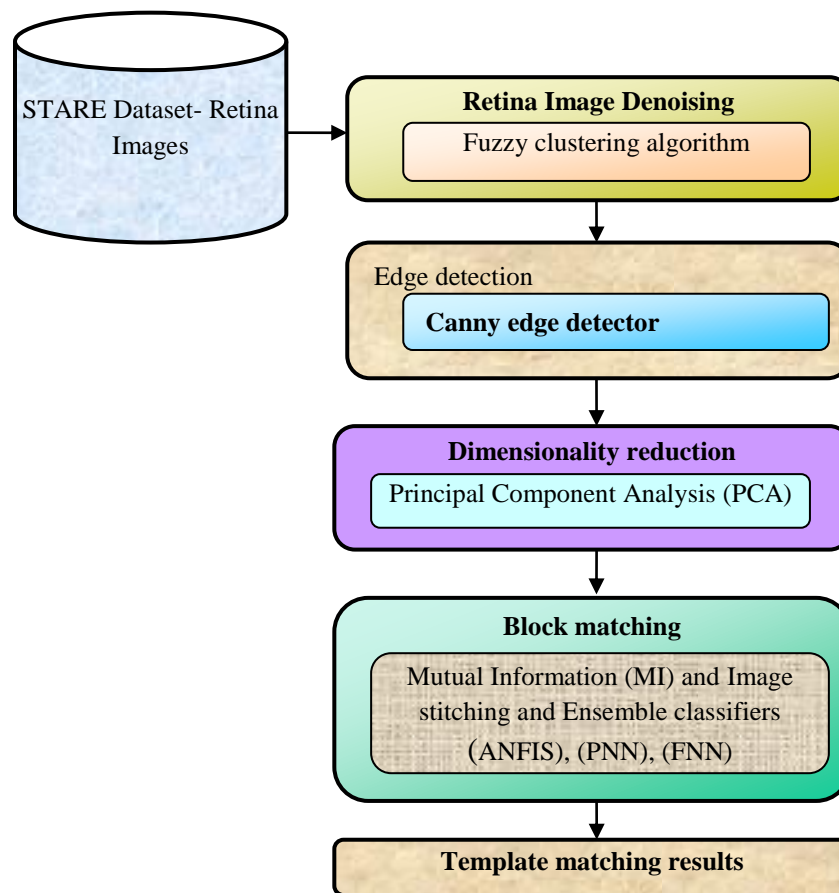


Figure: 1. Overall architecture of proposed work

3.1. Noise Removal Using Fuzzy Clustering

Retina Dataset: On STARE retinal dataset, synthetic deformations is used for testing suggested technique. An low cost adapter (< US\$ 400) based an optical system D-eye is used for collecting vivo data. Comparison is made between different dimension reduction technique's performance on STARE dataset.

Proposed retina picture's flowchart is displayed in Figure 2. Fuzzy clustering usage is denounced in this. Identification phase defines effective removal of noises.

Noisy pixel location can be effectively computed using proposed detection algorithm, which leads to enhanced miss detection rate and false alarm rate. Using clustering technique, independent clustering of low intensity and high intensity pixels are done. In noise-free group, majority of pixels are clustered. In this noise removal approach, in two steps, accomplished the impulse noise detection. Noisy pixels are first located and noise-free pixel values are maintained in second phase as illustrated in figure 2.

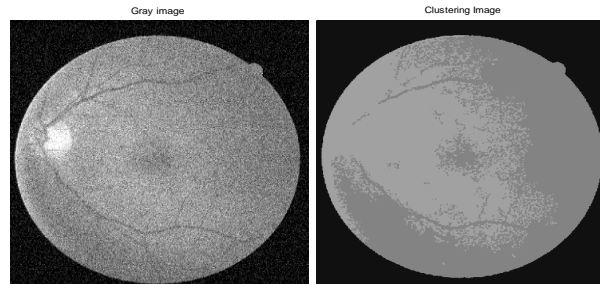


Fig.2. Fuzzy Clustering Noise removal

The step by step process of Image denoising process:

Process I: Noisy pixels Location detection

1. A window size $M \times N$ is selected which is centred on retina image's every pixel.
2. Assume $p(i, j)$ as central pixel where window is centred. Central pixel's neighbourhood values are divided using FCM algorithm as two clusters.
3. Assume C_1 and C_2 are the two clusters formed by applying FCM. In every cluster, maximum value present after cluster formation are computed.
4. There are $M \times N = X$ values in window. These X values are divided using FCM algorithm into two clusters unsupervisedly. Assume m_1 and m_2 as two maximum values in these clusters.
5. In ascending order, from every cluster, values of m_1 and m_2 are sorted, so that $m_1 < m_2$.
6. Central pixel $p(i, j)$ is checked as noisy or noise free using following expression.

$$p(i, j) = \begin{cases} \text{noise} & \text{if } p(i, j) \leq m_1 \\ \text{noisefree} & \text{if } m_1 < p(i, j) \leq m_2 \end{cases} \quad (1)$$

Where, pixels with lowest intensity pixels are represented as m_1 and corresponds to noisy pixel, pixels with highest intensity pixels are represented as m_2 and corresponds to noise free pixels.

7. A pixel is left unaltered, if it lies in a noise free cluster.
8. In second detection stage, pixel is processed if it is a noisy one.

Process II: Location of noisy pixels detection

9. Now window size is changed to $U \times V$
10. Until satisfying stopping criteria, steps 3-7 are repeated in same manner.
11. In second stage also, if a pixel is detected as a noisy one, then it is marked as noisy pixel. In other cases, it is marked as noise free.
12. Well-known median filter is used for performing noisy pixel's restoration. Computed the neighbouring pixels median value within $U \times V$ window size and noisy pixel values are replaced using this.

In next step, for edge detection process, these noise removed pixels are given as an input.

3.2. Edges detection using canny edge detection operator

In object identification, retina images edge identification is major step. Traditional single threshold technique enhancement is represented by canny operator, where based on image histogram's gradient, low

and high threshold values are selected. Without some pre-specified information, edge locating is done using edge detection algorithms [14,15].

Hysteresis based edge tracking, double threshold, non-maxima suppression, gradient direction and magnitude computation and image filtering and smoothing are the five basic canny edge detection algorithm steps. Different Gaussian kernels are used for smoothening the image.

Edges at gray level intensity changes are high are computed using Canny algorithm after smoothing. Image gradients are selected for locating these regions. Sobel operator is used for computing every pixel's gradient and following kernels are used for approximating x and y's gradient directions.

$$K(G_x) = \begin{pmatrix} -1 & 0 & 1 \\ -2 & 0 & 2 \\ -1 & 0 & 1 \end{pmatrix} \quad (2)$$

$$K(G_y) = \begin{pmatrix} 1 & 2 & 1 \\ 0 & 0 & 0 \\ -1 & -2 & -1 \end{pmatrix} \quad (3)$$

Then Euclidean distance is computed via gradient magnitude.

$$|G| = \sqrt{G_x^2 + G_y^2} \quad (4)$$

Extension of edges are happen sometimes and because of this, accurate computation of this is not possible. So, edge direction needs to be computed for solving this problem.

$$\theta = \arctan \frac{|G_x|}{G_y} \quad (5)$$

Blurred edges are converted into sharp edges using this. For this, local maxima are maintained and all other points are rejected. Following procedure is followed for every pixel.

- Gradient direction is rounded to nearest 45°, according to 8 nearest neighbours' usage.
- Current pixel's edge strength is compared with pixel in negative and positive gradient direction's edge strength. Comparison is made with current pixel's south and north pixel's if direction is north, i.e. 90.
- Pixel value will be preserved if current pixel's edge strength is high, else pixel value is suppressed.

Based on intensity value, marked the preserved pixels. Real edges points are represented by most of these pixels. But, these pixels may be created because of color variation or noise. In order to detect and remove false edge pixels, two thresholds namely higher and lower threshold are used by Canny algorithm. Strong pixels corresponds to pixels value greater than higher threshold and pixel values less than smaller threshold are eliminated.

Weak pixels are marked on the pixels having value between two thresholds. Reliable edges corresponds to strong edges and in final result they are included immediately. Weak edges having connection with strong edges only included in final result.

3.3.PCA for Location Estimation And Mutual Information

This section presents a mutual knowledge based image registration and dimensionality reduction combination. After image denoising, constructions of low-dimensional summaries are enabled using dimension reduction techniques while eliminating data redundancies and noise.

In 2d space, template location is estimated by duplicating full image dimension, hence template's coarse location is added with dimensional reduction techniques. In this section, Retina Match dimension reduction technique is selected as PCA.

Full image corresponds to mosaic image of D-eye images or broad-field fundus image .In specific, new variable range are created by PCA using input variable's weighted linear combination. Afterwards, for multimodal images, specified the MI maximization.

Full image corresponds to mosaic image of D-eye images or wide-field fundus image. Optimizer used for maximizing MI is formed form the technique utilized by Newton. A quasi-concave function is formed from MI function and only near convergence, valid results are produced by Newton's method parabolic theorem.

After performing initial transformation on cost functions convex portion, optimization is induced for divergence by this. Displacement's good configuration is provided by suggested coarse localization for maximizing MI's cost function in a subsequent manner.

Optimum value computation is similar to this and within MI metric's convex domain, it drops and highly efficient optimization is provided by this. Extreme positions are avoided. For coarse position, blocking PCA and PCA are used at first, which is a basic concept and it is a warm beginning for pursuing proper registration as illustrated in figure 3.

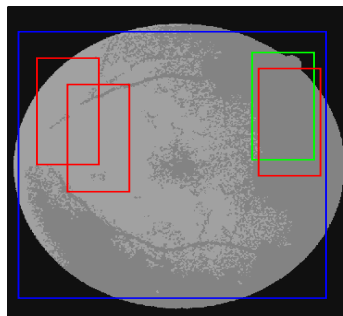


Fig.3.PCA and Coarse Localization

For accurate registration, configured the MI metric for discovering optimum transformation. High efficiency and precision can be achieved using accurate registration after reducing optimization domain to a narrow range near to optimum position with respect to coarse localization. Coarse location is shown in figure 5.

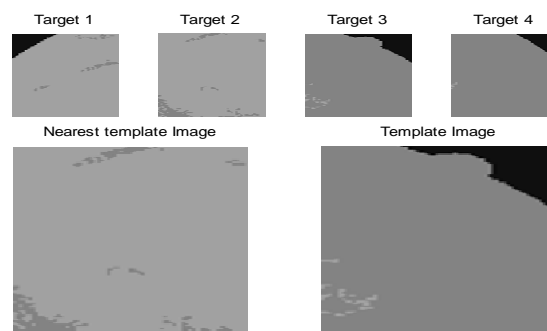


Fig.4.The coarse localization with nearest target image

3.4. Proposed Template Matching using ensemble classifiers

From PCA, all images will be stitched for template matching using image registration process and MI. For producing enhanced diseases detection accuracy, high resolution pictures are required.

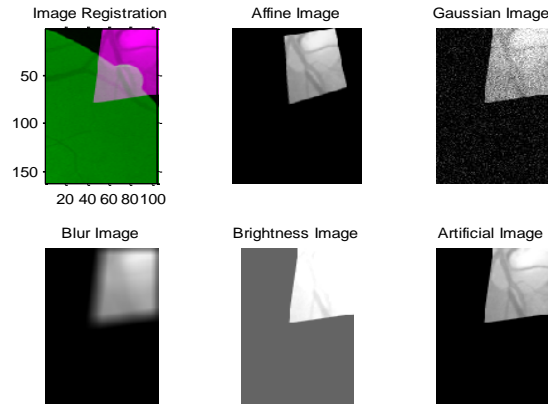


Fig.4. Image Registration

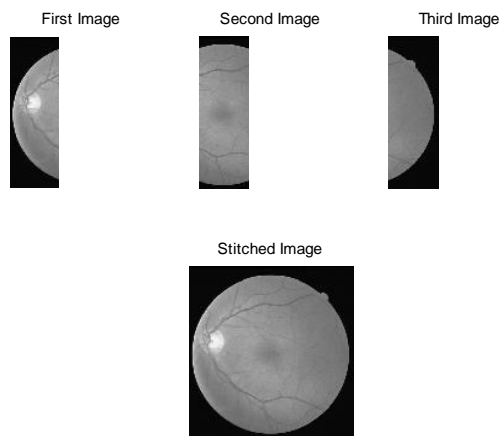


Fig.5. Image Stitching

Ensembling

The idea behind all get-together put together systems is that with respect to the remote possibility that solitary classifiers or features are different, by then they can make different bungles, and uniting these models can lessen the slip-up through averaging. Group learning is essentially used to improve request or figure execution, where a singular model doesn't have these capacities; especially in overseeing multiclass issues.

In an ensemble, for consolidating individual system's consequences, there are various techniques. Ballot and averaging are casted using two normally utilized techniques. In Boosting gathering, averaging performs superior to casting a ballot.

1. N specialists are generated with its own underlying qualities. (from an appropriation, starting qualities are typically picked arbitrarily)
2. Every master is trained independently.
3. Specialists are combined and their qualities are normalized.

Averaging strategy where ith classifier is resolved in a following manner.

Where, for specified information x_i , ideal yield vector is given by $d(x)$ and from i th arrange, genuine yield vector is represented as $f_i(x)$. In all classifier, on first call, picture is marked as not affected or affected. For affected images, disease grade is provided by call. Cotton wool spots are given as input parameters and removed the vein pixels. Using these two parts, for trained images, models can be build using this and test time's clear classification can be done.

3.4.1. Adaptive Neuro Fuzzy Inference System (ANFIS)

Selected features are given as an input to ANFIS. ANFIS is a type of neural network and its performance is based on neuro fuzzy network. Figure 6 shows the ANFIS architecture implementation [16].

Nodes in principal layer are adaptive. Input's fuzzy membership grade are produced at the output of layer 1 and is expressed by,

$$O_i^1 = \mu_{A_i}(x) \text{ for } i = 1, 2 \quad (6)$$

Where, x and y represents input nodes, linguistic labels are given by A and B , memberships functions are given by, $\mu_A(x)$ and $\mu_B(y)$, and they assumes a bell shaped curve where, highest value equal to 1 and lowest value equals to 0.

$$\mu(x) = \frac{1}{1 + \left(\frac{x - c_i}{a_i}\right)^{2b_i}} \quad (7)$$

Here, a_i , b_i , and c_i are the premise parameters set.

Fixed nodes are there in the subsequent layer and are marked with M . It indicates that, they are used as a simple multiplier. Output of this layer is given by,

$$O_i^2 = w_i = \mu_{A_i}(x) \mu_{B_i}(y), \quad i = 1, 2 \quad (8)$$

Rule's firing strength is represented using output w_i . Each and every node's results represent it.

Third layer nodes are fixed and are marked with N . This demonstrates that, normalization role is assumed by them to previous layer firing strengths. This layer output is represented using following condition.

$$O_i^3 = w_i = \frac{w_1}{w_1 + w_2}, \quad i = 1, 2 \quad (9)$$

These layer consequences are termed as normalized firing strengths.

Nodes in fourth layer are adaptive. Each and every node's output corresponds to first order polynomial for a first order Surgeon model and normalized firing strength. This layer output is given by this condition.

$$O_i^4 = w_i f_i = w_i(p_i x + q_i y + r_i) \quad (10)$$

Where, layer 3 output is indicated as w , parameter set is given by $\{p_i, q_i, r_i\}$ and are termed as resultant parameters.

There is only a single fixed node termed as S in fifth layer. Every single approaching signal is summed using this node. So, model's general output is expressed as,

$$O_i^5 = \sum_{i=1} w_i f_i = \frac{\sum_i w_i f_i}{\sum_i w_i} \quad (11)$$

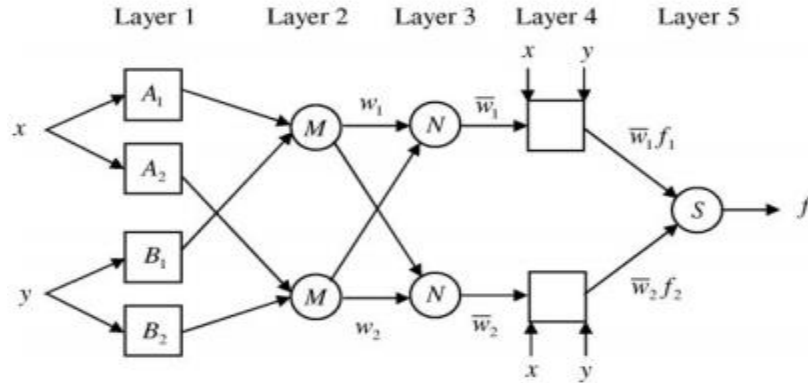


Figure.6. ANFIS architecture

Thus, an adaptive network is produced with practically identified reason to exist using a Sugeno first-order fuzzy inference system. The ANFIS is streamlined using a modified consequent parameters and antecedent parameters. Subsequently, specific objective function's end goal can be minimized.

3.4.2. Probabilistic neural network (PNN)

For opportunistic spectrum access, Probabilistic neural network is introduced using cognitive radio. In this work, without creating any interference to primary users, best suitable secondary users are selected for accessing available spectrum. According to below mentioned three antecedents so called descriptors, they are collected [17]. Descriptors are given by,

Ant 1 defines efficiency of Spectrum Utilization

Ant 2 defines mobility Degree

Ant 3 defines Distance between Secondary user and PU.

There are three layers in PNN.

Input Layer: It has input nodes and input data.

Pattern layer: Probability functions are there in second layer and for computing input probability, train set points are utilized as centers and probability density function are used for this computation.

Output layer: Voting, largest value selection, output generation are performed in third layer. Then computed the associated class label.

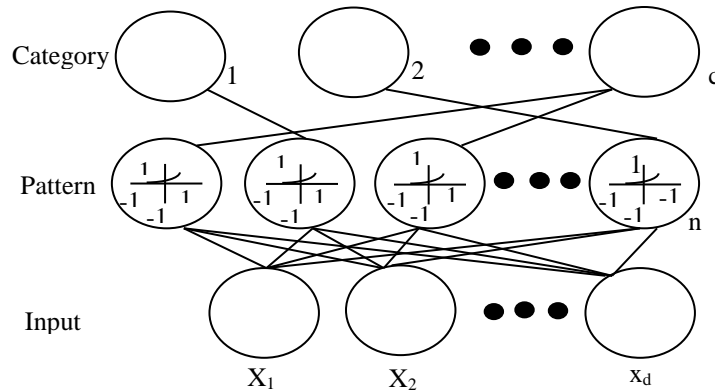


Figure: 7. Structure of PNN

A well-known Bayesian classifier techniques forms base for this PNN fundamental and it is utilized in various classical pattern-recognition systems. For every classification class, class-dependent probability density functions are constructed using Parzen windows which is a nonparametric estimation approach. For input including secondary user distance to PU, Mobility degree, spectrum utilization efficiency, probability of x belonging to class A is estimated using Parzen and it is given by probability density function.

$$F_A(x) = \frac{1}{(2\pi)^{m/2} \sigma^m} \sum_{i=1}^n \exp \left[-\frac{(x-x_j)^T (x-x_j)}{2\sigma^2} \right] \quad (12)$$

Where, input vector with m dimension is represented as x , pattern number is given by j , for a category A, j th training pattern is represented as x_j , training patterns count is given by n , input space dimension is given by m , adjustable “smoothing parameter is given by σ .”

Specified pattern vector’s probability belonging to specific category is computed using these probability density functions. Category with highest probability value is assigned with an input. Less training time is needed in PNN and it is possible to implement adaptation to new patterns via modification of training databases using new patterns and its correct classes.

Thus, according to highest probability, spectrum are accessed by secondary user. In general, with the constraint of no interference to primary user, spectrum can be accessed by a secondary user having largest distance from primary user or it can be accessed by secondary user having maximum spectrum utilization efficiency.

4.3.3. Fuzzy neural network (FNN)

Fuzzy neural network is used in this work. Implicit knowledge representation is a major shortcoming of neural network. Heuristic and subjective nature is exhibited by fuzzy logic systems. In a trial and error technique, fuzzy rules are determined, output and input scaling factors are determined and membership functions are selected. Huge time is required for designing fuzzy logic system.

The fuzzy logic systems robustness is integrated with neural network’s learning capabilities for rectifying, these fuzzy logic systems and neural networks drawbacks. In network structure, fuzzy logic concepts are embedded using this integration.

In a uniform fashion, both linguistic information in IF–THEN rules form and numerical information in input/output pairs form are combined using a natural framework provided by this [18,19].

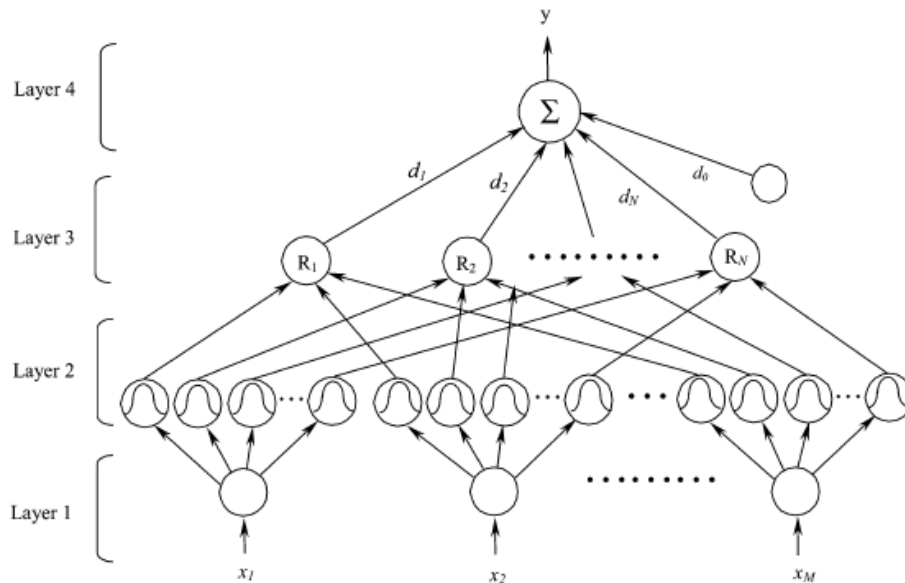


Fig.8. Structure of the four-layered fuzzy neural network

There are four layers in Fuzzy neural network,

Layer 1- Input layer: In this layer, computations are not performed. One input variable corresponds to every node of this layer and input values are transmitted to next layer directly, which is given by,

$$\mathbf{o}^{(1)} = \mathbf{a}_i^{(1)} = x_i \quad (13)$$

Where FNN's input variables are represented as $x_i, i = 1, 2, \dots, M$.

Layer 2—Membership function layer: A membership function is represented using every node of this layer and it represents any one of the input variable's linguistic label like slow, fast, etc. In can also be stated that, in Layer 2, membership value which specifies degree to which an input value belonging to a fuzzy set.

$$\mathbf{o}^2 = \mathbf{u}_i^{(j)} \left(\mathbf{a}_i^{(2)} \right) \quad (14)$$

Where, membership function is represented as $\mathbf{u}_i^{(j)}(\cdot): \mathbf{R} \rightarrow [0, 1], i=1,2,\dots,M, j=1,2,\dots,N$. In this layer, performed operation using Gaussian membership function is given by,

$$\mathbf{o}^{(2)} = e^{-\left(\frac{(\mathbf{a}_i^{(2)} - m_{ij})^2}{\sigma_{ij}^2} \right)} \quad (15)$$

Where, i^{th} input variable x_i 's j^{th} term's Gaussian membership function width or variance is represented as σ_{ij} and mean or center are represented as m_{ij} .

Layer 3—Rule layer: One fuzzy rule in this represented using a node in this layer and rule's precondition matching is performed using this. For every Layer 2 node, AND operation is used.

$$\mathbf{o}^{(3)} = \prod_{i=1}^M \mathbf{a}_i^{(3)} = e^{-[D_j(x-m_j)]^T} [D_j(x - m_j)] \quad (16)$$

Where, $D_j = \text{diag}\left(\frac{1}{\sigma_{1j}}, \dots, \dots, 1/\sigma_{Mj}\right)$, $m_j = [m_{1j}, m_{2j}, \dots, m_{Mj}]^T$ $X = [x_1, x_2, \dots, x_M]^T$ FNN input vector. Corresponding fuzzy rule's firing strength is represented using Layer-3 node's output.

Layer 4—Output layer: In this layer, single node $o^{(4)}$ is labeled using Σ , all input signals summation is computed as overall output in this layer.

$$o^{(4)} = \sum_{j=1}^N d_j \times a_j^{(4)} \times d_o \quad (17)$$

Where, Layer 4's output action strength having association with Layer 3 rule corresponds to connecting weight and scalar is a bias.

5. Results and Discussion

In Retina match and ASIFT, retinal images are used for performing experimental results between four matching techniques. On 400 source fundus images with sick and strong retinas, from STARE dataset, retrieved the full fundus images. After making affine transformation to parallelogram from square, on mapping on random selection, a full fundus image is hold by every pair.

Square template is obtained by square mapped cropping in this area along with warping. For 12 images, in FOV template images, attained 200×200 pixels size. The 10% of full image is used as a template dimension. For five image classes like Artificial, Brightness, Blur, Gaussian and Affine, analysis of developed MI-Ensemble classifiers (MI-ENCLA) Mutual Information output is done with respect to available techniques like MI-ISVM, IR-MI and MI. Figure 9 shows the Nearest Template and retina image with Target Image input.

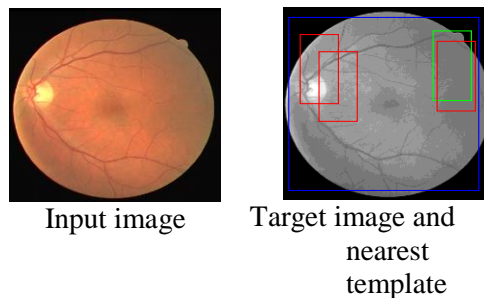


Fig.9. Retina image with Target Image and Nearest Template

Table:1. Performance comparison results of various techniques

Metrics	MI	IR-MI	MI-SVM	CA-EN
Affine	63	7.5	85.5	89
Gaussian	52.5	81	90	93
Blur	70	81	90	92.7
Brightness	63	81	90	93
Artificial	70	90	94.5	96.2

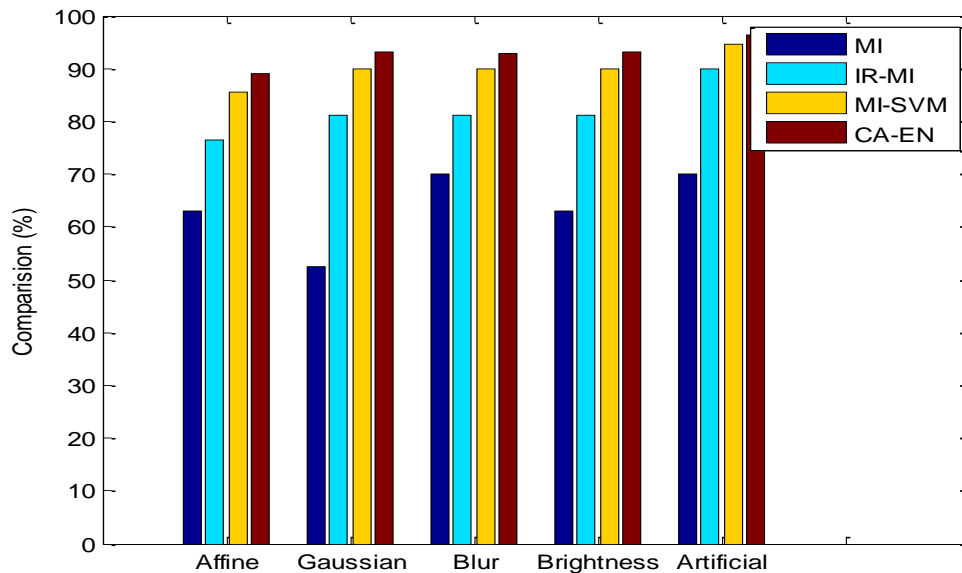


Figure:10.Different retina images matching Comparison vs. Classifiers

Above figure shows the matching comparison of artificial, brightness, blur, Gaussian and affine images produced by available MI-ISVM, IR-MI and MI and newly introduced **MI- ENCLA** Retina template recognition techniques. Image edges are detected in this proposed work by performing edge tracking based on double threshold via hysteresis and different Gaussian kernels are used for smoothing it.

The retina disease recognition performance's mean error is reduced using this kernel technique. Higher artificial, brightness, blur, Gaussian and Affine results are produced by proposed **MI- ENCLA** technique while low artificial, brightness, blur, Gaussian and Affine results are produced by available techniques like MI-ISVM, IR-MI and MI as indicated in that results. For affine image, around 89% accuracy results are produced by proposed **MI- ENCLA**, but only 85.5% is produced by MI-ISVM, 75% is produced by IR-MI and 63% is produced by MI.

6. Conclusion and Future Work

The retinal fundus images are classified as healthy or diseased using a developed system. A retina template matching system is developed using ensemble of fuzzy neural network (FNN), Probabilistic neural network (PNN) and Adaptive Neuro Fuzzy Inference System (ANFIS) classifiers. This binary classification is done successfully using this system. To train as well as to test, retinal fundus images are derived from STARE dataset.

Fuzzy clustering is used in this developed system for denoising the images and dimensionality reduction is performed using PCA via MI and at last, ensemble techniques are used for recognizing images as a healthy or affected one. In future, this model can be enhanced for learning specific diseases and test images can be labelled respectively. A huge as well as different datasets are required for this purpose and for multi-class labeling, model should be trained accordingly.

References

1. Galdran, A., Chakor, H., Alrushood, A.A., Kobbi, R., Christodoulidis, A., Chelbi, J., Racine, M.A. and Benayed, I., 2019. Automatic classification and triage of diabetic retinopathy from retinal images based on a convolutional neural networks (CNN) method. *Acta Ophthalmologica*, 97.
2. Wang, Y., Zhang, J., An, C., Cavichini, M., Jhingan, M., Amador-Patarroyo, M.J., Long, C.P., Bartsch, D.U.G., Freeman, W.R. and Nguyen, T.Q., 2020, May. A Segmentation Based Robust Deep Learning Framework for Multimodal Retinal Image Registration. In *ICASSP 2020-2020 IEEE International Conference on Acoustics, Speech and Signal Processing (ICASSP)* (pp. 1369-1373). IEEE.
3. Ren, X., Zheng, Y., Zhao, Y., Luo, C., Wang, H., Lian, J. and He, Y., 2017. Drusen segmentation from retinal images via supervised feature learning. *IEEE Access*, 6, pp.2952-2961.
4. Zhang, M., Wang, J.Y., Zhang, L., Feng, J. and Lv, Y., 2019, March. Deep residual-network-based quality assessment for SD-OCT retinal images: preliminary study. In *Medical Imaging 2019: Image Perception, Observer Performance, and Technology Assessment* (Vol. 10952, p. 1095214). International Society for Optics and Photonics.
5. Praveen Sundar, P.V., Ranjith, D., Vinoth Kumar, V. et al. *Low power area efficient adaptive FIR filter for hearing aids using distributed arithmetic architecture*. *Int J Speech Technol* 23, 287–296 (2020).
6. Sheng, B., Li, P., Mo, S., Li, H., Hou, X., Wu, Q., Qin, J., Fang, R. and Feng, D.D., 2018. Retinal vessel segmentation using minimum spanning superpixel tree detector. *IEEE transactions on cybernetics*, 49(7), pp.2707-2719.
7. Ramzan, A., Akram, M.U., Ramzan, J., Salam, A.A. and Yasin, U.U., 2018, July. Automated Inner Limiting Membrane Segmentation in OCT Retinal Images for Glaucoma Detection. In *Science and Information Conference* (pp. 1278-1291). Springer, Cham.
8. Imran, A., Li, J., Pei, Y., Akhtar, F., Yang, J.J. and Wang, Q., 2019, December. Cataract Detection and Grading with Retinal Images Using SOM-RBF Neural Network. In *2019 IEEE Symposium Series on Computational Intelligence (SSCI)* (pp. 2626-2632). IEEE..
9. Zhao, Y., Zheng, Y., Zhao, Y., Liu, Y., Chen, Z., Liu, P. and Liu, J., 2018, September. Uniqueness-driven saliency analysis for automated lesion detection with applications to retinal diseases. In *International Conference on Medical Image Computing and Computer-Assisted Intervention* (pp. 109-118). Springer, Cham.
10. Vinoth Kumar V, Ramamoorthy S, Dhilip Kumar V, Prabu M, Balajee J.M., "Design and Evaluation of Wi-Fi Offloading Mechanism in Heterogeneous Network", *International Journal of e-Collaboration (IJeC)*, IGI Global, 17(1), 2020.
11. Pratap, T. and Kokil, P., 2019, March. Automatic Cataract Detection in Fundus Retinal Images using Singular Value Decomposition. In *2019 International Conference on Wireless Communications Signal Processing and Networking (WiSPNET)* (pp. 373-377). IEEE.
12. Raman, M., Korah, R. and Tamilselvan, K., 2019. An automatic localization of optic disc in low resolution retinal images by modified directional matched filter. *Int. Arab J. Inf. Technol.*, 16(1), pp.1-7.
13. Barua, B. and Hasan, M.M., 2016, September. A new approach of detection and segmentation of blood vessels for the classification of healthy and diseased retinal images. In *2016 3rd International Conference on Electrical Engineering and Information Communication Technology (ICEEICT)* (pp. 1-6). IEEE.
14. Ali, D. and Das, A., 2019, January. Face Detection and Eye Extraction using Canny Edge Detection and Hough Transform. In *Proceedings of conference on Advancement in Computation, Communication and Electronics Paradigm (ACCEP-2019)* (p. 14).
15. Tahmid, T. and Hossain, E., 2017, December. Density based smart traffic control system using canny edge detection algorithm for congregating traffic information. In *2017 3rd International Conference on Electrical Information and Communication Technology (EICT)* (pp. 1-5). IEEE.
16. Baghaee, H.R., Mirsalim, M., Gharehpetian, G.B., Talebi, H.A. and Niknam-Kumle, A., 2017. Notice of violation of IEEE publication principles: A hybrid ANFIS/ABC-based online selective harmonic elimination switching pattern for cascaded multi-level Inverters of microgrids. *IEEE Transactions on Industrial Electronics*.
17. Nor, A.F.M., Sulaiman, M., Kadir, A.F.A. and Omar, R., 2017. Voltage stability analysis of load buses in electric power system using adaptive neuro-fuzzy inference system (ANFIS) and probabilistic neural network (PNN). *ARPN Journal of Engineering and Applied Sciences*, 12(5), pp.1406-1410.
18. Gao, Y., Liu, J., Wang, Z. and Wu, L., 2019. Interval type-2 FNN-based quantized tracking control for hypersonic flight vehicles with prescribed performance. *IEEE transactions on systems, man, and cybernetics: systems*.
19. Gao, M., Li, Y., Dobre, O.A. and Al-Dhahir, N., 2018. Joint blind identification of the number of transmit antennas and MIMO schemes using Gerschgorin radii and FNN. *IEEE Transactions on Wireless Communications*, 18(1), pp.373-387.